coatings

MDPI

Article

Response of Optically Transparent pH Sensing Films to Temperature and Temperature Variations

Daniela M. Topasna * and Gregory A. Topasna

Department of Physics and Astronomy, Virginia Military Institute, Lexington, VA 24450, USA; topasnaga@vmi.edu

* Correspondence: topasnadm@vmi.edu

Received: 30 September 2019; Accepted: 24 December 2019; Published: 26 December 2019

Abstract: There are numerous applications for thin films based chemical pH sensors, in such areas as biomedical, military, environmental, food, and consumer products. pH sensitive films fabricated through the ionic self-assembled monolayers technique were made of polyelectrolyte polyallylamine hydrochloride and the water-soluble organic dye molecule Direct Yellow 4. The films were monitored in various environmental conditions and for selected periods, at temperatures varying between −13.7 and 46.2 °C. Absorbance measurements and atomic force microscopy performed before and after thermal treatment indicate that for optimized thickness and composition the films maintain their functionality and are not affected by long-term exposure at these temperatures.

Keywords: thin films; optical pH sensors; ionic self-assembled monolayer; layer-by-layer assembly; dyes

1. Introduction

Numerous studies have demonstrated the advantages of using thin films for sensing applications, and more so for optical sensing in biomedical, food, environmental, and industrial fields [1,2]. Depending on the deposition method these films can be applied either over large areas, or confined spaces, or be included in fiber optic sensors [3–6]. They are durable, fast, low cost, lightweight, compact, maintenance free, and multifunctional. In addition, they display electromagnetic immunity, they are stable within a wide temperature range, and are suitable for remote sensing. In healthcare, for example, the common temperature range of interest is 35 to 45 °C [7], with some applications that require extension of this range to 20–80 °C.

Ionic self-assembled monolayers (ISAM) or a layer-by-layer (LBL) technique has been used extensively and efficiently to fabricate a variety of functional thin films to include small molecules, polymers, nanoparticles, fullerenes, quantum dots, DNA, etc. [8–11]. The ISAM technique is environmentally friendly, allows for control of film structure and thickness at the nanometer level, and creates uniform and homogenous films. In addition, it is very simple and inexpensive. Bilayer thickness is controlled through the parameters (concentration, pH, salt content) of the electrolyte solutions used in the fabrication process. Optically transparent pH sensing films fabricated by the ISAM technique have additional unique properties, as they can be conformal and multifunctional [6]. Such thin films based sensors whose properties allow use over a wide range of temperatures are well sought after in the food industry [12] as well as for remote accessible locations.

Previous reports of ISAM optical pH sensing films include various combinations of polyelectrolytes or polyelectrolytes and dyes, such as poly(diallyldimethylammonium chloride) (PDDA) and poly(acrylic acid) (PAA) [13], poly(allylamine hydrochloride) (PAH) and P-Azo [14], Prussian Blue [15], and Neutral Red [16,17]. In addition, these films have been incorporated and analyzed in optical fiber pH sensors. However, few of these films have been studied at high temperatures, up to 100 °C, where degradation of the dye or of the film can occur. [14,18,19]. Little information exists about

the large area morphology at temperatures other than room temperature. To our knowledge, there have not been reports of studies of such films exposed at low temperatures, especially at or below freezing temperatures.

In our study we characterized over a range of temperatures ionically self-assembled thin films designed for pH optically transparent sensors. Absorbance measurements and atomic force microscopy (AFM) studies show that the films do not lose their mechanical integrity and remain functional after exposure to such environments for which the temperatures ranged from −13.7 °C as the lowest to 46.2 °C the highest for this experiment. This temperature range is of importance in the food industry, specifically 4–60 °C, over which bacteria growth is significant [20]. Storage below freezing point is also of interest in the food industry and for biomedical samples as these types of films could find applications as smart coatings [21–23]. Our films are based on poly(allylamine hydrochloride) (PAH) and Direct Yellow 4 (also known as Brilliant Yellow) (DY). Direct Yellow 4 is an azo direct dye whose optical properties (absorbance) are pH dependent [24]. At low pH values and up to pH 6.6 the solution has a yellow color, with absorption peak near 400 nm. As pH increases above 6.6 to 7.9 the color of the solution turns orange with absorption peak shifted at 495 nm and at around pH 9.0 the solution turns to orange-red. The dye has the isosbestic point at 436 nm [25].

2. Materials and Methods

2.1. Materials

PAH/DY films were fabricated from aqueous solutions using the layer-by-layer (LbL) technique which yields ionic self-assembled monolayers. Poly(allylamine hydrochloride) (PAH), MW 70,000 from Aldrich (Milwaukee, WI, USA), Direct Yellow 4 (also known as Brilliant Yellow) purchased from Sigma Aldrich (St. Louis, MO, USA), NaCl and HCl from Fisher Scientific (Atlanta, GA, USA) were used as received. The chemical structures of PAH and DY4 are shown in Figure 1. The films were deposited on cleaned microscope glass slides (Fisher Scientific, Atlanta, GA, USA) [26].

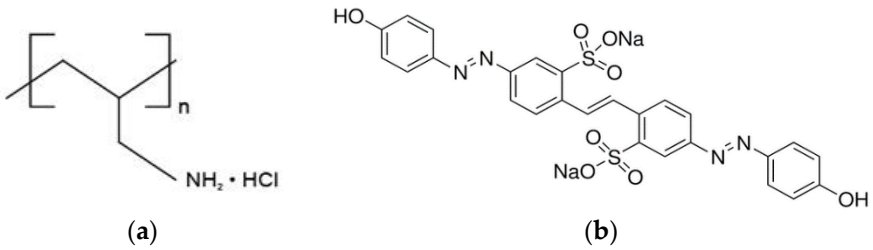

(**a**) (**b**)

Figure 1. Chemical structures for (**a**) poly(allylamine hydrochloride) (PAH) and (**b**) Direct Yellow 4 (from Sigma Aldrich).

2.2. Solutions

Ultrapure water (Barnstead™ E-Pure™ Ultrapure Water Purification System, Dubuque, IA, USA) with resistivity 18.2 MΩ·cm was used to prepare solutions and for the intermediate rinsing. Polyelectrolyte solution for PAH was prepared in a concentration of 10 mM with respect to the monomer unit. Its pH was adjusted to 3.86 using a Fisher Scientific Accumet AB 15 pH meter (Fisher Scientific, Suwanee, GA, USA). Direct Yellow (DY) was prepared in a solution of 0.18 mM and with a pH adjusted to 3.20. Both solutions had 150 mM NaCl. Rinsing was done with deionized water at a pH of 5.22.

2.3. Film Assembly

The films were fabricated by the ionic self-assembled monolayers technique (ISAM) using a StainMate Max (Fisher Scientific, Suwanee, GA, USA) programmable automated stainer. The clean substrate is first immersed in the polycation solution, PAH, then rinsed with deionized water to remove any excess material. The procedure is repeated with anion solution, DY, and then rinsed again. These

steps yield one bilayer, PAH/DY. The step sequence for film fabrication process of one PAH/DY bilayer is listed in Table 1. This sequence is repeated until the desired number of bilayers is reached. Using results from previous studies, the films were fabricated with a PAH cap layer [18,19,24,27]. This final layer has been demonstrated to protect and extend functionality of the film as a pH sensor when immersed in high pH values up to 8.7. For our study, the films have a maximum of 6 bilayers of PAH/DY and a final PAH layer. The notation for this is $(PAH/DY)_{6.5}$. After film deposition, the slides were dried using prepurified nitrogen.

Table 1. Step sequence of one bilayer (PAH/DY) film fabrication.

Staining Process for PAH/DY (1 Bilayer)						
Step	**Bath #**	**Solution**	**Time (s)**	**Agitation**	**Time Over Bath (s)**	**Agitation**
1	1	PAH Solution	300	N	5	Y
2	2	DI Water	30	Y	5	Y
3	3	DI Water	30	Y	5	Y
4	6	DI Water (flowing)	30	Y	5	Y
5	10	DY Solution	300	N	5	Y
6	9	DI Water	30	Y	5	Y
7	8	DI Water	30	Y	5	Y
8	6	DI Water (flowing)	30	Y	5	Y

2.4. Characterization Methods

Absorbance measurements were obtained using a Lambda 900 Perkin Elmer UV-VIS-NIR spectrophotometer (Shelton, CT, USA) and Ocean Optics STS-VIS Miniature Spectrometer (Dunedin, FL, USA).

2.5. Atomic Force Microscopy (AFM)

Atomic Force Microscopy imaging was performed in air at an ambient temperature before and after thermal treatments using Agilent Technologies 5500 AFM/SPM (Englewood, CO, USA). AFM measurements were made in noncontact mode [28] (Acoustic AC Mode) using Nanosensors^{TM} probes (NanoAndMore USA Corporation, Watsonville, CA, USA) with tip radius <10 nm, spring constant 48 N/m, and resonant frequencies between 143 kHz and 157 kHz. Several scan areas were investigated of which we report the 500 nm × 500 nm and 10 μm × 10 μm.

3. Results and Discussion

The uniform buildup of ISAM layers is demonstrated by the linear increase of absorbance with the number of deposited bilayers as shown in Figure 2 for films with 2, 4, 6, and 6.5 bilayers. The $(PAH/DY)_{6.5}$ film ends with the transparent PAH cap layer.

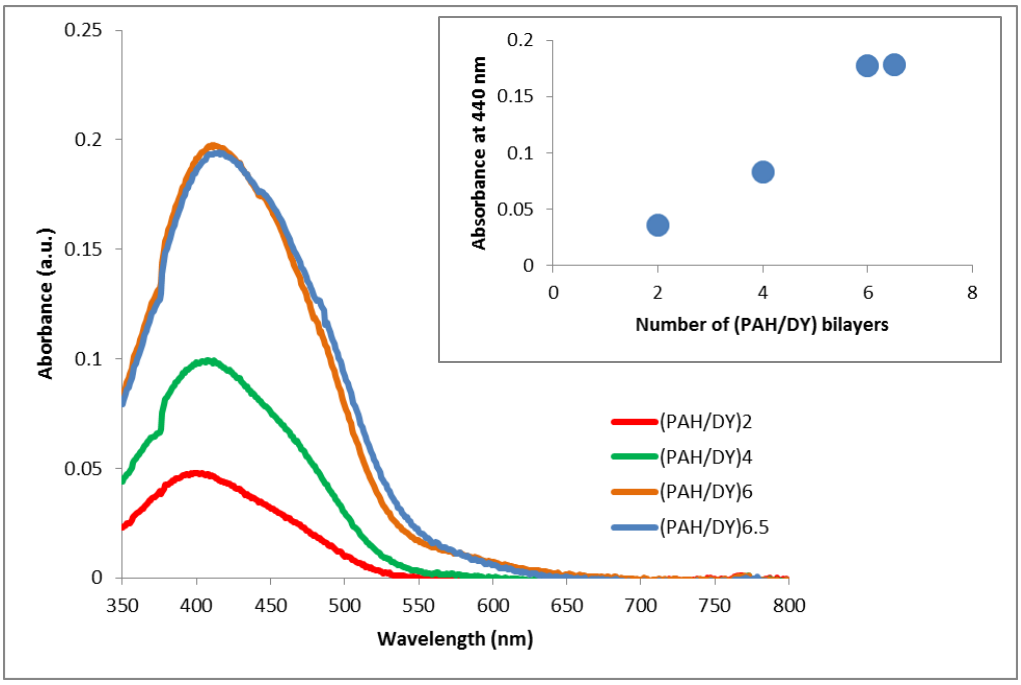

Figure 2. Absorbance spectra of various (PAH/DY) films. Inset shows absorbance versus number of bilayers.

After fabrication the films were kept for specific periods (24, 16, and 1 h) at various temperatures: −13.7, 3.3, and 46.2 °C respectively. In Figure 3, glass slides coated with PAH/DY films display uniform buildup and homogeneous coverage.

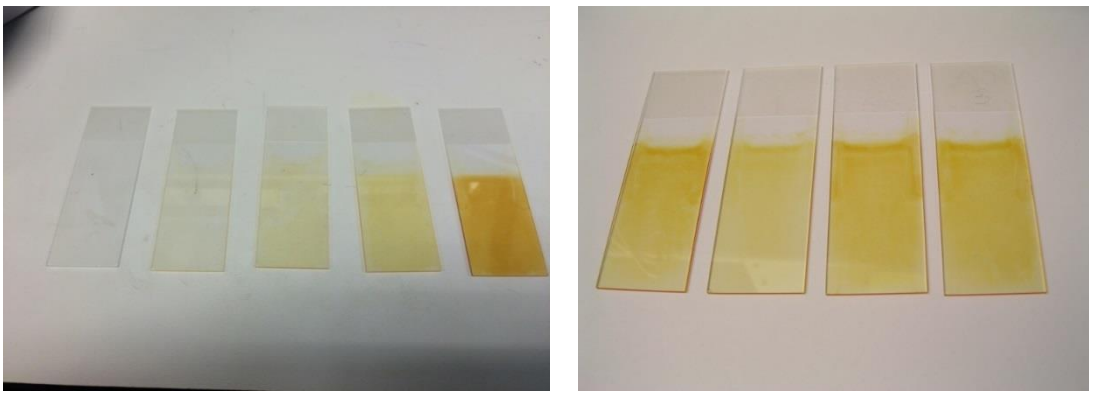

(**a**) (**b**)

Figure 3. ISAM films display homogeneity. Left photo: blank slide and (PAH/DY) films with 2, 4, and 6 bilayers (from left to right). The final slide has 6 bilayers with an additional PAH cap that protects films at high pH levels. Right photo includes $(PAH/DY)_{6.5}$ films (from left to right) before thermal treatment, and after thermal treatment at 46.2, 3.3, and −13.7 °C.

Figure 4 displays film absorbance recorded at 440 nm versus treatment temperatures. The results show that absorbance, and therefore film thickness, does not change significantly as the film is heated or cooled. It also indicates that the dye remains in the film after thermal treatment, maintaining its functionality.

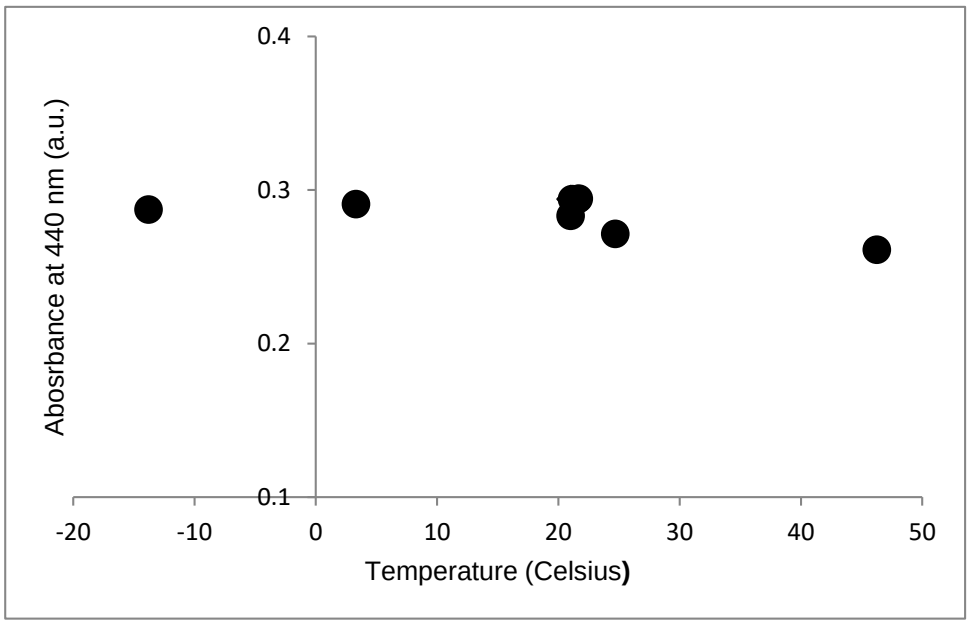

Figure 4. Normalized absorbance of films during thermal treatment at 46.2, 3.3, and −13.7 °C.

The films were characterized by atomic force microscopy in air at an ambient temperature before and after thermal treatment. Figure 5 displays 10 μm × 10 μm AFM images taken before and immediately after heating or cooling of $(PAH/DY)_{6.5}$ films. Common characteristics of all films under study are uniform and continuous coverage of the substrate over a large area. In addition, mechanical integrity remains after thermal treatment with no apparent defects, cracks, or other surface damage. Roughness and root mean square roughness values are shown in Table 2. The variations in roughness values between the two different scanned areas are common and have been reported in the literature [28]. Higher roughness at low temperatures could be due to condensation on the film surface. Lower roughness values at the higher temperature suggest that polymer chains are allowed to relax into a more flat morphology.

Table 2. Surface roughness of $(PAH/DY)_{6.5}$ on glass.

	Average Roughness (nm)		**Root Mean Square Roughness (nm)**	
Temperature (°C)	**10 μm × 10 μm**	**500 nm × 500 nm**	**10 μm × 10 μm**	**500 nm × 500 nm**
−13.3	7.36	9.59	9.45	12
3.3	7.44	7.22	9.6	8.76
21	8.37	7.52	10.8	9.32
46.2	5.46	5.71	6.95	7.04

Images of $(PAH/DY)_{6.5}$ films taken over a 500 nm × 500 nm scanned area also confirm that film coverage is not affected by thermal treatment as seen in Figure 6 for films treated at 46.2, 3.3, and −13.7 °C. The films have measured values for roughness of 7.0 nm for the films heated at 46.2 °C, 8.8 nm for the films cooled at 3.3 °C, and 12.0 nm for those exposed to below freezing temperature of −13.7 °C. It is notable that films exposed to subfreezing temperatures also remained smooth and do not show cracks after thermal exposure, although they were fabricated from aqueous solutions.

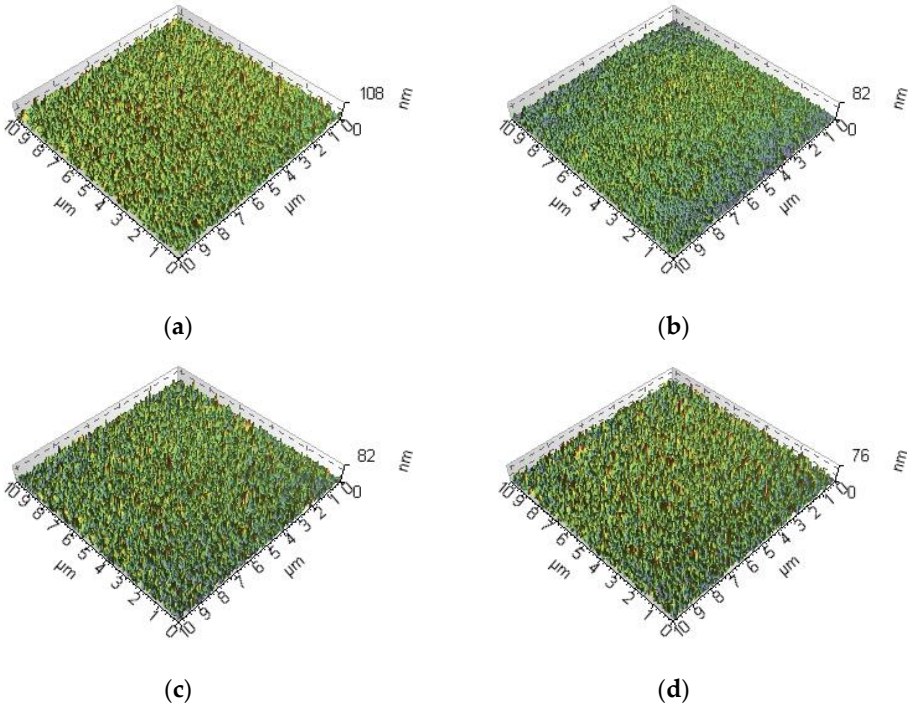

Figure 5. AFM images of $(PAH/DY)_6PAH$ films before and after thermal treatment. (**a**) Before thermal treatment; (**b**) after heating for 1 h at 46.24 °C; (**c**) after low temperature exposure for 16 h at 3.31 °C; (**d**) after low temperature exposure (freezing) for 24 h at −13.7 °C.

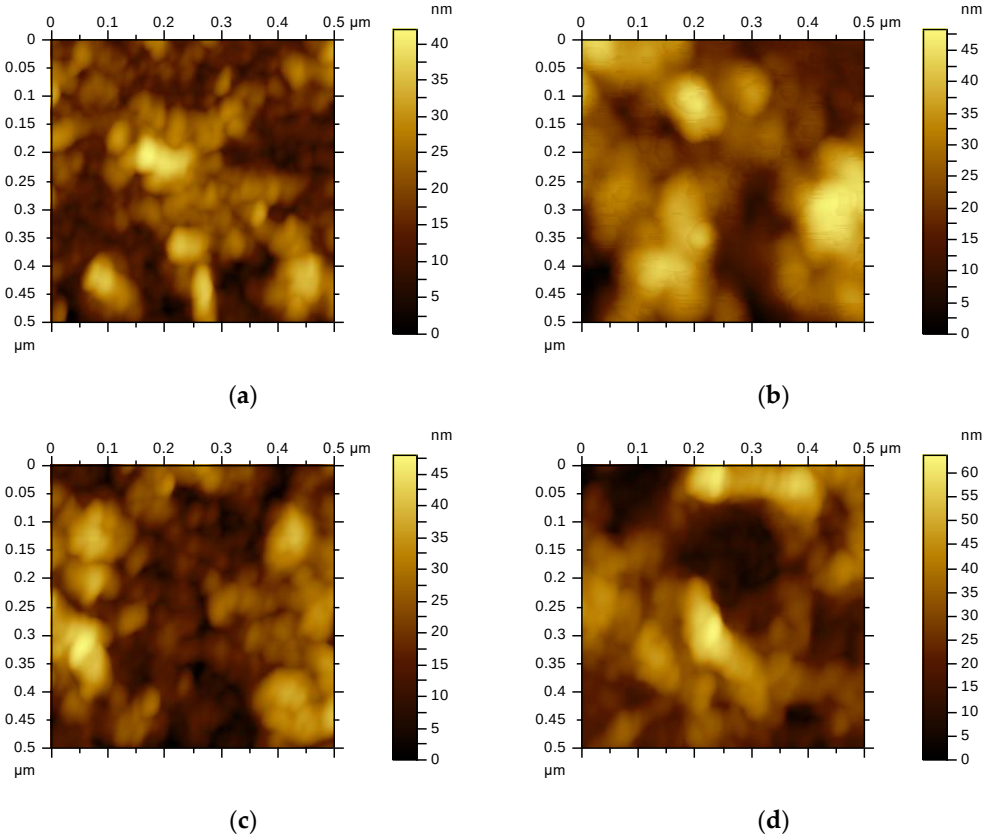

Figure 6. AFM images of $(PAH/DY)_6PAH$ films over a 500 nm × 500 nm scanned area (**a**) before thermal treatment and after thermal treatments at (**b**) 46.2 °C (**c**) at 3.3 °C, and (**d**) at −13.3 °C. All films display continuous film coverage free of defects.

AFM images are in agreement with other reports on ISAM films [13] where a grain like morphology was observed. Based on the ionic strength of the dipping solutions films could have a smooth or vermiculate morphology. We used solutions with 150 mM salt concentration which is well below the threshold of 1.0 M NaCl at which vermiculate morphology could occur. Grain size observed in our films is approximately 50 nm, which has been observed previously in similar films. [29,30]. Also in agreement with other studies [13] is the higher roughness values for ISAM films with a lower number of bilayers. The films are smooth and free of defects, unlike spin coated films of PVP and DY where the presence of the dye generated pores and depressions and increased roughness [31].

4. Conclusions

We fabricated pH sensitive PAH/DY optically transparent films using ISAM method. Films show continuous and uniform buildup of layers. For specific material combination and thickness in $(PAH/DY)_{6.5}$ sample, we characterized the films before and after exposure to a range of temperatures, from −13.3 to 46.2 °C. Optical absorbance measurements indicate that the dye remains in the film upon thermal treatment and that optical properties of the films are not altered. AFM analysis indicates that surface of films remains smooth, unchanged, and is not affected by long term exposure to these temperatures, even exposure to temperatures below freezing. Root mean square roughness values for the films are comparable after thermal exposures, with values between 7.0 and 12.0 nm.

Author Contributions: Conceptualization, methodology, investigation, D.M.T.; writing—original draft preparation, D.M.T.; writing—review and editing, D.M.T. and G.A.T. All authors have read and agreed to the published version of the manuscript.

Funding: This research was partially funded by VMI Grants-in-Aid of Research Jackson Hope Fund, VMI Faculty Development, and VMI Wetmore Fund.

Conflicts of Interest: The authors declare no conflicts of interest.

References

1. Bastarrachea, L.J.; Wong, D.E.; Roman, M.J.; Lin, Z.; Goddard, J.M. Active Packaging Coatings. *Coatings* **2015**, *5*, 771–791. [CrossRef]
2. Wencel, D.; Abel, T.; McDonagh, C. Optical chemical pH sensors. *Anal. Chem.* **2014**, *86*, 15–29. [CrossRef] [PubMed]
3. Wolfbeis, O.S. Chemical Sensing Using Indicator Dyes. In *Optical Fiber Sensors*; Dakin, J., Culshaw, B., Eds.; Artech House: Boston, MA, USA, 1997; Volume IV, pp. 53–107.
4. Krohn, D.A.; MacDougall, T.; Mendez, A. *Fiber Optic Sensors: Fundamentals and Applications*, 4th ed.; SPIE Press: Bellingham, WA, USA, 2014; pp. 233–253, 307–310.
5. Rivero, P.J.; Goicoechea, J.; Arregui, F.J. Optical Fiber Sensors Based on Polymeric Sensitive Coatings. *Polymers* **2018**, *10*, 280. [CrossRef] [PubMed]
6. Rivero, P.J.; Goicoechea, J.; Arregui, F.J. Layer-by-layer nano-assembly: A powerful tool for optical fiber sensing applications. *Sensors* **2019**, *19*, 683. [CrossRef] [PubMed]
7. Correia, R.; James, S.; Lee, S.-W.; Morgan, S.P.; Korposh, S. Biomedical application of optical fibre sensors. *J. Opt.* **2018**, *20*, 073003. [CrossRef]
8. Decher, G. Fuzzy Nanoassemblies: Toward Layered Polymeric Multicomposites. *Science* **1997**, *277*, 1232–1237. [CrossRef]
9. Decher, G. Layer-by-Layer Assembly (Putting Molecules to Work). In *Multilayer Thin Films: Sequential Assembly of Nanocomposite Materials*, 2nd ed.; Decher, G., Schlenoff, J.B., Eds.; Wiley-VCH Verlag GmbH & Co. KGaA: Weinheim, Germany, 2012; Volume 1, pp. 10–13.
10. Marciu, D.; Miller, M.; Ritter, A.L.; Murray, M.A.; Neyman, P.J.; Graupner, W.; Heflin, J.R.; Wang, H.; Gibson, H.W.; Davis, R.M. Efficiency optimization in ionically self-assembled thin film polymer light-emitting diodes. In *Light-Emitting Diodes: Research, Manufacturing, and Applications IV*; Yao, H.W., Ferguson, I.T., Schubert, E.F., Eds.; Proceedings of SPIE: Bellingham, WA, USA, 2000; Volume 3938. [CrossRef]

11. Figura, C.; Neyman, P.J.; Marciu, D.; Brands, C.; Murray, M.A.; Hair, S.; Davis, R.M.; Miller, M.; Heflin, J.R. Thermal stability and immersion solution dependence of second-order nonlinear optical ionically self-assembled films. In *Organic Photonic Materials and Devices II*; Bradley, D.D.C., Kippelen, B., Eds.; Proceedings of SPIE: Bellingham, WA, USA, 2000; Volume 3939, pp. 214–222.
12. Bae, E.; Bhunia, A.K. Nano-Optical Sensors for Food Safety and Security. In *Optochemical Nanosensors*, 1st ed.; Cusano, A., Arregui, F.J., Giordano, M., Cutolo, A., Eds.; CRC Press: Boca Raton, FL, USA, 2013; pp. 497–512.
13. Shao, L.-Y.; Yin, M.-J.; Tam, H.-Y.; Albert, J. Fiber optic pH sensor with self-assembled polymer multilayer nanocoatings. *Sensors* **2013**, *13*, 1425–1434. [CrossRef] [PubMed]
14. Mermut, O.; Barrett, C.J. Stable sensor layers self-assembled onto surfaces using azobenzene-containing polyelectrolytes. *Analyst* **2001**, *126*, 1861–1865. [CrossRef] [PubMed]
15. Corres, J.M.; Matias, I.R.; del Villar, I.; Arregui, F.J. Design of pH Sensors in Long-Period Fiber Gratings Using Polymeric Nanocoatings. *IEEE Sens. J.* **2007**, *7*, 455–463. [CrossRef]
16. Goicoechea, J.; Zamarreño, C.R.; Matías, J.R.; Arregui, F.J. Optical fiber pH sensors based on layer-by-layer electrostatic self-assembled Neutral Red. *Sens. Actuators B Chem.* **2008**, *132*, 305–311. [CrossRef]
17. Raoufi, N.; Surre, F.; Sun, T.; Grattan, K.T.V.; Rajarajan, M. Improvement of Optical Properties of pH- sensitive Nanolayers Coating Deposited using Layer-by-Layer Technique. In Proceedings of the 2012 IEEE SENSORS, Taipei, Taiwan, 28–31 October 2012; pp. 1–4.
18. Raoufi, N.; Surre, F.; Rajarajan, M.; Sun, T.; Grattan, K.T.V. Optical sensor for pH monitoring using a layer-by-layer deposition technique emphasizing enhanced stability and re-usability. *Sens. Actuators B Chem.* **2014**, *195*, 692–701. [CrossRef]
19. Topasna, D.M.; Topasna, G.; Liu, M.; Tseng, C.H. Conformal self-assembled thin films for optical pH sensors. In *Nanosensors, Biosensors, and Info-Tech Sensors and Systems 2016*; Varadan, V.K., Ed.; Proceedings of SPIE: Bellingham, WA, USA, 2016; Volume 9802, p. 98021Q.
20. Fletcher, B.; Mullane, K.; Platts, P.; Todd, E.; Power, A.; Roberts, J.; Chapman, J.; Cozzolino, D.; Chandra, S. Advances in meat spoilage detection: A short focus on rapid methods and technologies. *CyTA J. Food* **2018**, *16*, 1037–1044. [CrossRef]
21. Lee, S.B.; Clabaugh, K.C.; Silva, B.; Odigie, K.O.; Coble, M.D.; Loreille, O.; Scheible, M.; Fourney, R.M.; Stevens, J.; Carmody, G.R.; et al. Assessing a novel room temperature DNA storage medium for forensic biological samples. *Forensic Sci. Int. Genet.* **2012**, *6*, 31–40. [CrossRef] [PubMed]
22. Olisekodiaka, M.J.; Onuegbu, A.J.; Ebesunun, O.M.; Agbedana, E.O.; Taylor, G.O. Effects of Storage Temperature, pH and Time on Urinary Albumin Level. *Afr. J. Biomed. Res.* **2011**, *14*, 73–75.
23. Vernekar, N.V.; Jabannavar, V.B. Effect of storage and temperature on two biochemical analytes (creatinine and urea) in pooled serum samples stored at −20 °C. *Indian J. Health Sci. Biomed. Res.* **2017**, *10*, 63–67. [CrossRef]
24. Egawa, Y.; Kayashida, R.; Anzai, J. Multilayered Assemblies Composed of Brilliant Yellow and Poly(allylamine) for an Optical pH Sensor. *Anal. Sci.* **2006**, *22*, 1117–1119. [CrossRef] [PubMed]
25. Haynes, W.M. (Ed.) *CRC Handbook of Chemistry and Physics*, 91st ed.; CRC Press (Taylor and Francis Group): Boca Raton, FL, USA, 2010.
26. Iler, R.K. *The Chemistry of Silica: Solubility, Polymerization, Colloid and Surface Properties, and Biochemistry*; John Wiley & Sons: New York, NY, USA, 1979; pp. 624–629.
27. Fujita, S.; Shiratori, S. The initial growth of ultra-thin films fabricated by a weak polyelectrolyte layer-by-layer adsorption process. *Nanotechnology* **2005**, *16*, 1821–1827. [CrossRef]
28. Lobo, R.F.M.; Pereira-da-Silva, M.A.; Raposo, M.; Faria, R.M.; Oliveira, O.N., Jr. The morphology of layer-by-layer films of polymer/polyelectrolyte studied by atomic force microscopy. *Nanotechnology* **2003**, *14*, 101–108. [CrossRef]
29. Raposo, M.; Lobo, R.F.M.; Pereira-da-Silva, M.A.; Faira, R.M.; Oliveira, O.N., Jr. Thickness and roughness measurements in poly(o-methoxyaniline) layer-by-layer films using AFM. In Proceedings of the 10th International Symposium on Electrets, Athens, Greece, 22–24 September 1999; pp. 533–536.

30. Lobo, R.F.M.; Pereira-da-Silva, M.A.; Raposo, M.; Faria, R.M.; Oliveira, O.N., Jr. In situ thickness measurements of ultra-thin multilayer polymer films by atomic force microscopy. *Nanotechnology* **1999**, *10*, 389–393. [CrossRef]
31. Chaplanova, Z.D.; Murauski, A.A.; Rogachev, A.A.; Agabekov, V.E.; Gracheva, E.A. Multi-Layered Anisotropic Films Based on the Azo Dye Brilliant Yellow and Organic Polymers. *J. Appl. Spectrosc.* **2013**, *80*, 658–662. [CrossRef]